Design of a Voice Coil Motor Used in the Focusing System of a Digital Video Camera

Hsing-Cheng Yu[1], Tzung-Yuan Lee[2], Shyh-Jier Wang[1], Mei-Lin Lai[1], Jau-Jiu Ju[1], Der-Ray Huang[1], and Shir-Kuan Lin[2]

[1]OES/ITRI, Hsinchu 310, Taiwan, R.O.C.

[2]Department of Electrical and Control Engineering, National Chiao Tung University, Hsinchu 300, Taiwan, R.O.C.

This paper raises a valid method to design a voice coil motor (VCM) used in the focusing system of a digital video camera (DVC). A better VCM performance, such as lower battery consumption, higher efficiency, and shorter focusing time, can be achieved by turning the diameter of a winding coil, the thickness of the magnet, and the winding spaces in a VCM.

Index Terms—**Battery consumption, digital video camera, focusing, voice coil motor.**

I. Introduction

RECENTLY, digital video cameras (DVCs) have been very popular, and better performance of focusing is always asked. In order to attract more customers, the conventional focusing actuators, steppers, in a DVC are gradually replaced with a voice coil motor (VCM), whose focusing time is shorter. Most works concerning VCMs considered mainly the dynamic response [1]. However, both the battery consumption and the efficiency of a VCM are also important factors to be taken into account in a DVC system, since DVCs are portable apparatuses. This paper tries to introduce a design procedure for a VCM that meets the strict requirements of low power consumption, high efficiency, and fast focusing.

II. Problematic Formulations

A typical VCM used in a DVC consists of a permanent magnet, a moving coil, a yoke, and a steel plate as shown in Fig. 1. The design problem of a VCM restricted in a limited space ($l_x \times l_y \times l_z$) can be formulated to find the diameter of one coil in the windings ϕ and the thickness ratio γ

$$\gamma = \frac{l_m}{l_w} \tag{1}$$

where l_m is the thickness of the permanent magnet and l_w is the thickness of the windings. Indeed, the magnetic field in the VCM is constructed by determining γ. Furthermore, the number of turns of the moving coil N can be estimated as

$$N \approx \text{round}\left(\frac{l_w}{\phi}\right) \cdot \text{round}\left(\frac{l_p}{\phi}\right) \tag{2}$$

where l_p is the width of the windings and N is a function of γ and ϕ.

The design philosophy for a high-quality VCM used in a DVC is to define three performance indexes, namely: 1) the rising time t_r; 2) the battery consumption energy E_o; and 3) the efficiency η. The rinsing time is a measure of the focusing time of a DVC, while the battery consumption energy is that of the battery duration. The efficiency is used to estimate the copper loss of the VCM. These indexes are formulized as

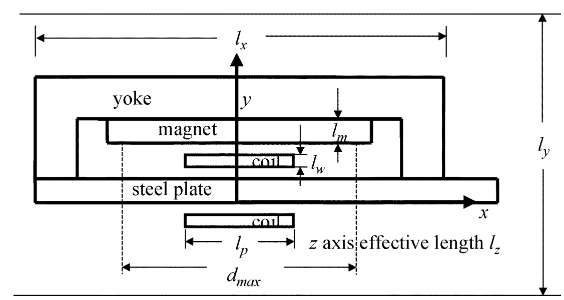

Fig. 1. Structures of the VCM in DVC.

$$d_{\max} = \int_0^{t_r} v(t)\mathrm{d}t \tag{3}$$

$$E_o(\gamma,\phi) = \int_0^{t_r} i(t)V(t)\mathrm{d}t \tag{4}$$

$$\eta(\gamma,\phi) = \frac{E_o(\gamma,\phi) - \int_0^{t_r} i^2(t)R(\gamma,\phi)\mathrm{d}t}{E_o(\gamma,\phi)} \tag{5}$$

where $d_{\max}$ is the maximum stroke of the VCM, v is the speed of the VCM moving part, i is the current of the windings per turn, V is the terminal voltage, and R is the coil resistance. Equations (3), (4) and (5) show that t_r, E_o, and η are all functions of γ and ϕ. The design goals are to decrease t_r and E_o and to increase η to obtain a better VCM.

It is known [2] that the dynamic equations of the VCM can be written as

$$V(t) = i(t)R(\gamma,\phi) + L(\gamma,\phi)\frac{\mathrm{d}i(t)}{\mathrm{d}t} + K_v(\gamma,\phi)v(t) \tag{6}$$

$$m\frac{\mathrm{d}v(t)}{\mathrm{d}t} + B_m v(t) = F_e(\gamma,\phi) - F_L = K_f(\gamma,\phi)i(t) - F_L \tag{7}$$

where L is the coil inductance, K_v is the voltage constant, m is the mass of the VCM moving part, B_m is the damping constant, F_e is the electric force, F_L is the loading force, and K_f is the force constant. If V, R, L, K_f, K_v, B_m, $d_{\max}$, m, and F_L are

Digital Object Identifier 10.1109/TMAG.2005.855161

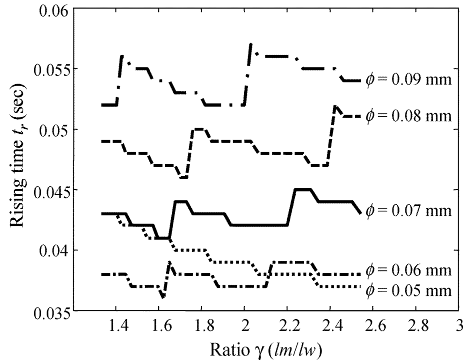

Fig. 2. Plots of t_r related to ϕ and γ.

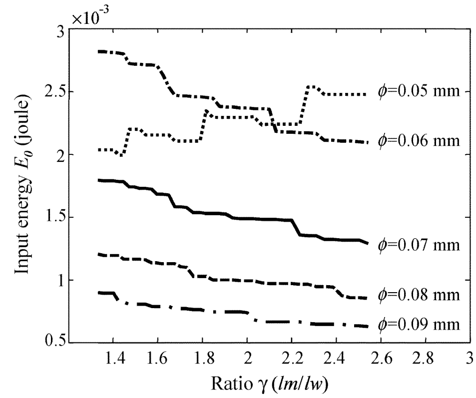

Fig. 3. Plots of E_o related to ϕ and γ.

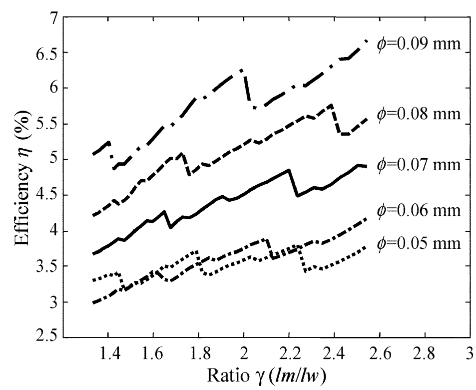

Fig. 4. Plots of η related to ϕ and γ.

known, $v(t)$ and $i(t)$ can be obtained by solving the two differential equations (6) and (7). Thus, the indexes t_r, E_o, and η can be evaluated by (3)–(5).

K_f can be written as

$$K_f = \frac{F_e}{i} \tag{8}$$

where F_e can be calculated by the Maxwell stress method [3]. It was pointed out [4] that the value of K_v is equal to K_f in the MKS unit. The coil inductance can be calculated by the perturbation of the energy stored in the magnetic field as [5]

$$L = \frac{W(i-\Delta i) - 2W(i) + W(i+\Delta i)}{(\Delta i)^2} \tag{9}$$

where W is the magnetic energy and Δi is the perturbation coil input current. In the design procedure, K_f, K_v, and L can then be predicted by the three-dimensional (3-D) finite element method.

From the Ohm's law, the coil resistance can be estimated as

$$R = \frac{\rho N l_t(\gamma)}{\frac{\pi\phi^2}{4}} \tag{10}$$

where ρ is the resistivity of the windings and l_t is the length of one turn in the windings. It should be remarked that K_f, K_v, R, and L are all functions of γ and ϕ, i.e., they vary with γ and ϕ.

III. Design Procedure

Given that m is 2.0 g, the maxima of V and i are 2.97 V and 30 mA, respectively, B_m is 0.005 Nt/(m/s), $d_{\max}$ is 5.21 mm, and F_L is 0.05 gw. As γ and ϕ vary, the finite element method and (8)–(10) are used to obtain K_f, K_v, R, and L. The values are substituted into (6) and (7) to solve for $v(t)$ and $i(t)$, which allow us to evaluate t_r, E_o, and η by (3)–(5). The relations of t_r, E_o, and η to γ and ϕ are then obtained and shown in Figs. 2, 3, and 4, respectively.

Fig. 2 reveals that t_r decreases with the decrease of ϕ and is affected little by γ. It follows from Fig. 3 that E_o decreases with the increases of both ϕ and γ with the exception of $\phi = 0.05$. On the contrary, η increases with the increase of both ϕ and γ. The maximum efficiency is $\eta = 6.7\%$ when $\gamma = 2.55$ and $\phi = 0.09$ mm.

The requirement of low t_r and E_o and high η forces us to choose $\gamma = 2.5$ and $\phi = 0.07$ mm, since $\phi \geq 0.08$ mm makes t_r too high to be acceptable. This design choice has $\eta \approx 4.9\%$, $E_o \approx 1.3 \times 10^{-3}$ J, and $t_r \approx 44$ ms. The rising time is only 1/6th as short as a conventional stepper.

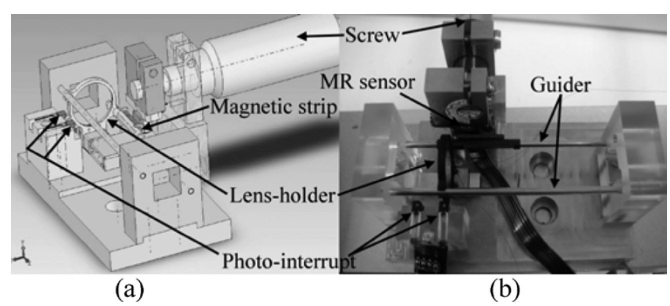

Fig. 5. VCM manufactured by OES. (a) Computer-aided design (CAD)/computer-aided manufacturing (CAM) simulation. (b) Materialization.

IV. Implementation and Experiments

A VCM with $\gamma = 2.5$, $\phi = 0.07$ mm, $N = 288$, and $m = 1.8$ g was manufactured and its photo is shown in Fig. 5. We assembled a lens holder for carrying an optical focusing lens and the coils of the VCM together. Two photo-interrupts (PIs)with the constant interval $d_{\max} = 5.21$ mm are set to detect t_r of the VCM. Furthermore, a magnetic strip with a 0.8-mm polar pitch is mounted on the lens holder and the magnetoresistive (MR) sensor is used to pick up the magnetic signals from the magnetic strip, so that the moving positions of the VCM can be obtained.

In the first step, we measured the impedance of the VCM by using an R–L–C meter to obtain $R = 32.8\,\Omega$ and $L = 1.2$ mH.

As regards the measurement of K_f and F_L, we know that

$$F = K_f i - F_L \tag{11}$$

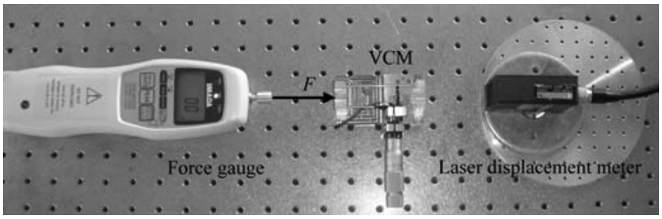

Fig. 6. Experimental system to measure K_f.

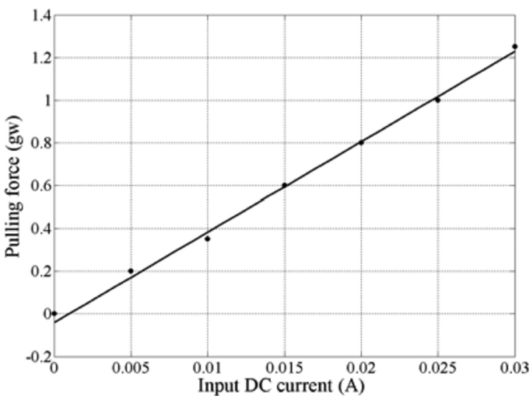

Fig. 7. Characteristics of the VCM pulling force.

where F is the net pulling force of the VCM. The experimental system is shown in Fig. 6, in which the force gauge and the lens holder are bound together with a thin wire. The force gauge measured F for several different direct current (dc) levels of 0, 5, 10, 15, and 30 mA applied to the VCM. The results are plotted in Fig. 7. It is worth mentioning that we should fix the position to measure the pulling force, so that F_L can be regarded as a constant. Therefore, a laser displacement meter was also installed in the experiment system to help us adjust the measurement position. Fig. 7 shows that F is indeed a linear function of i, and the results are consistent with (11). Consequently, it follows from (11) and Fig. 7 that K_f and F_L are 42.3 gw/A and 0.04 gw, respectively.

The output signals of the two PIs provide a way to measure t_r. Note that both PIs are disabled by a shelter piece that is inserted to the lens holder while the VCM is moving, and the shelter piece is fixed on the moving part of the VCM and moves when current is applied to the VCM. As the shelter piece crosses over a PI, the output signal of the PI will change, i.e., PI1 from "Low" to "High" level and PI2 from "High" to "Low" level. In addition to these two signals, the input voltage V and the exciting current i are also measured at the same time and recorded as shown in Fig. 8. The time between the rising edge of PI1 signal to the falling edge of PI2 signal is exactly the rising time t_r. Channels 1 and 2 in Fig. 8 indicate that $t_r = 44.5\ \mathrm{ms}$. Notice that channels 3 and 4 in Fig. 8 show that V and i are maintained almost constant. Finally, we obtain $E_o = 1.9 \times 10^{-3}$ J and $\eta = 3.9\%$ by substituting t_r into (4) and (5).

The comparison of the experimental results with the design values for $\gamma = 2.5$ and $\phi = 0.07\ \mathrm{mm}$ is listed in Table I. It can be seen that the differences between them are small. This verifies the proposed design method.

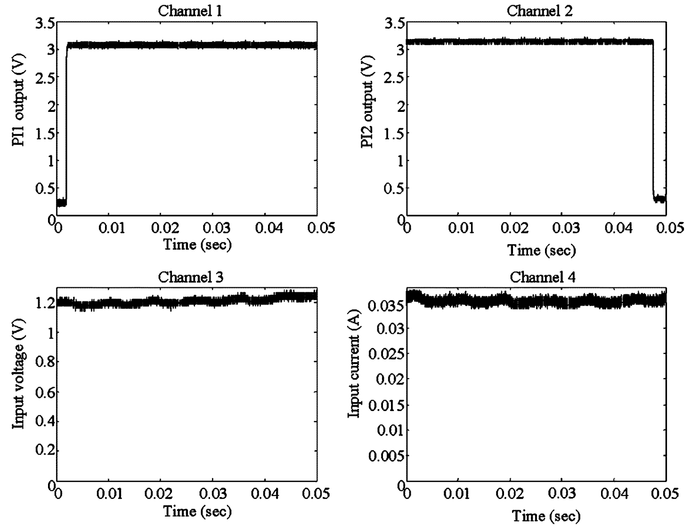

Fig. 8. Rising time t_r measurement.

TABLE I
COMPARISON WITH THE SIMULATED AND EXPERIMENTAL RESULTS

	Design values	Experimental results
R	34.8Ω	32.8Ω
L	1.3 mH	1.2 mH
K_f	42.9 gw/A	42.3 gw/A
t_r	44.0 ms	44.5 ms
E_o	1.3×10^{-3} joule	1.9×10^{-3} joule
η	4.9 %	3.9 %

V. CONCLUSION

This paper proposes a new design philosophy for a voice coil motor (VCM) used in the focusing system of a digital video camera (DVC). Three performance indexes are defined for the design goals of low power consumption, high efficiency, and fast focusing. A design procedure is proposed to achieve these goals by adjusting these three indexes. An example of designing and manufacturing VCM is also presented. Experimental results show that the measured performance indexes match the design values very well.

ACKNOWLEDGMENT

This work was supported by the Nano Technology Research Center at the Industrial Technology Research Institute.

REFERENCES

[1] S. Jang, J. Choi, S. Lee, H. Cho, W. Jang, and K. Jeong, "Analysis and experimental verification of moving-magnet linear actuator with cylindrical Halbach array," in *9th Joint Magnetism and Magnetic Materials/Int. Magnetics (MMM/Intermag) Conf.*, Anaheim, CA, 2004, BP-10.

[2] D. W. Novotny and T. A. Lipo, *Vector Control and Dynamics of AC Drivers*. New York: Oxford, 1996.

[3] D. A. Lowther and P. P. Silvester, *Computer-Aided Design in Magnetics*. New York: Springer-Verlag, 1986.

[4] E. P. Anderson and R. Miller, *Electric Motors*. Indianapolis, IN: T. Audel, 1983.

[5] N. A. Demerdash, "Determination of winding inductance in ferrite type permanent magnet electric machinery by finite elements," *IEEE Trans. Magn.*, vol. MAG-18, no. 6, pp. 1052–1054, Nov. 1982.

Manuscript received February 7, 2005.